Absorbing properties of atmospheric aerosol: analysis of microphysical optical characteristics

L.B. Letfulova, A.V. Starinov, and S.A. Beresnev

Ural State University, Ekaterinburg

Received December 25, 2000

The paper presents results of theoretical analysis of microphysical optical characteristics of atmospheric aerosol such as source function of electromagnetic energy absorbed in the particle volume, as well as absorption efficiency, absorption asymmetry, and radiation pressure factors. We present calculated results on these characteristics, obtained on the basis of Lorentz–Mie theory for different types of atmospheric aerosol, and discuss their dependence on the parameters influencing them. We intend to use these results for experimental study of dynamics of microparticles in the field of directed low-intensity radiation, mimicking the behavior of tropospheric and stratospheric aerosols.

Introduction

The systematic study of the processes of heating and fragmentation of liquid-droplet and solid atmospheric aerosol has a long history of already a few decades.[1–3] Also, many-year is the history of analysis of the evolution of aerosol particles in the low-intensity solar radiation field, including the phenomena of particle evaporation and motion under impact of different specific forces.

Theoretical analysis of the processes of heat and mass exchange of aerosols in the radiation field involves solution of three interrelated problems: (1) determination of the distribution of internal heat sources of electromagnetic origin ("electromagnetic problem"); (2) calculation of temperature field in the volume and on the surface of particle ("thermophysical problem"); and (3) analysis of finite evolutionary characteristics such as evaporation rate, photophoretic force, radiation pressure force, moment of force, particle momentum in the radiation field, etc. ("gas kinetics problem"). At least in its linear-intensity formulation, the electrodynamic problem can be treated practically independent of the second and third problems. This analysis should provide information on the inside-particle distribution of absorbed electromagnetic energy (source function $B(\mathbf{r})$), absorption efficiency factor (dimensionless absorption cross section) Q_{abs}, absorption asymmetry factor J_1, radiation pressure efficiency factor K_{rp} (all called here the particle microphysical optical characteristics that determine the particle absorbing properties).

The present work concentrates on theoretical analysis of electrodynamics problem, primarily aimed at gaining deeper insight into the specific features of behavior of tropospheric and stratospheric aerosols in the solar radiation field. The analysis includes (1) determination of the relationships among microphysical optical characteristics and gas kinetic parameters; (2) use of an efficient technique for calculation of these characteristics employing previously tested algorithms of Lorentz–Mie theory; and (3) discussion of their specific features for main atmospheric aerosol types as functions of parameters determining them. We intend to use these results for simulation of dynamics of atmospheric aerosol in the radiation field by the methods of electrodynamics suspensions and model thermophysical experiment.

Microphysical optical characteristics and gas kinetics parameters in the problems of aerosol evaporation and motion in the field of directed radiation

Suppose that a plane wave of monochromatic non-polarized radiation with the wavelength λ and intensity I is incident on a spherical particle of radius R_0 in gas. The particle has complex refractive index $m(\lambda) = n(\lambda) + ik(\lambda)$, assumed to be known for the given wavelength and, within the first approximation, temperature independent. The particle can either be solid or "volatile" (in the sense that phase changes can occur on its surface).

Radiation–particle interaction gives rise to electromagnetic energy sources distributed in the particle volume according to the *source function* $B(\mathbf{r})$ which, in the non-polarized, monochromatic, axially symmetric problem formulation, can be expressed as

$$B(r, \theta, \varphi) = \frac{1}{2\pi} \int_0^{2\pi} \frac{|E(r, \theta, \varphi)|^2}{E_0^2} \, d\varphi = B(r, \theta, \frac{\pi}{4}), \quad (1)$$

where $E(r, \theta, \varphi)$ is the local strength of the electric field inside a particle; while E_0 is the amplitude of the field strength in the incident wave. Depending on diffraction parameter $\rho = 2\pi R_0/\lambda$ and refractive index $m(\lambda)$, the electromagnetic energy may be distributed in

0235-6880/01/01 62-07 $02.00

the particle nonuniformly and in a complex way. The source function $B(r, \theta, \varphi)$ for a spherical (homogeneous or multilayer) particle can be calculated from Lorentz–Mie theory.[4–6] Moments of $B(r, \theta, \varphi)$ of different orders determine the main microphysical optical characteristics in the particle–radiation interaction process. In particular, the *absorption efficiency factor* Q_{abs} (the fraction of electromagnetic energy absorbed by the particle[7]) is

$$Q_{abs} = 4J_0 = 4nk\rho \int_0^{\pi} \sin\theta \, d\theta \times$$

$$\times \int_0^1 x^2 \, B(x, \theta, \phi = \frac{\pi}{4}) \, dx, \quad x = r/R_0. \qquad (2)$$

The absorbed energy gives rise to temperature inhomogeneity on the particle surface, usually characterized by the particle surface temperature asymmetry factor J_1 (or, more correctly, by the *absorption asymmetry factor*)[8]

$$J_1 = 3nk\rho \int_0^{\pi} \sin\theta \, P_1(\cos\theta) \, d\theta \int_0^1 x^3 \, B\left(x, \theta, \phi = \frac{\pi}{4}\right) dx, \qquad (3)$$

where $P_m(\cos\theta)$ are Legendre polynomials. The value J_1 lies in the range $-0.5 \le J_1 \le 0.5$, and its negative (positive) values indicate that the particle sunlit (dark) side is predominately heated. Geometrically, the asymmetry factor identifies the position of the gravity center of the internal heat sources in the particle.

The higher-order moments of source function $B(\mathbf{r})$ in the general case can be written as

$$J_m = (2m + 1) \, kn\rho \int_0^{\pi} \sin\theta \, P_m(\cos\theta) \, d\theta \times$$

$$\times \int_0^1 x^{m+2} \, B(x, \theta, \varphi) \, dx, \quad m \ge 2. \qquad (4)$$

Unlike the above equations, they have no clear physical interpretation. Possibly, they provide more exact values of the efficiency (for even m) and absorption asymmetry (for odd m), and can be considered as some analogs of central distribution moments in mathematical statistics.[9] Analysis of these characteristics will be continued below.

The *radiation pressure factor* $K_{rp}(\rho, m)$ can be calculated from absorption and scattering efficiency factors[7]

$$K_{rp} = Q_{abs} + Q_{sca} \, (1 - \langle\cos\theta\rangle), \qquad (5)$$

where θ is the scattering angle. The radiation pressure force is an important factor in a number of low-intensity cases,[8] and it can be written as

$$F_{rp} = K_{rp}(\rho, m) \, \pi \, R_0^2 \, |E_0|^2/(8\pi). \qquad (6)$$

If particles interact with non-monochromatic radiation, a distinction must be made between spectral and broadband characteristics of the above quantities. In particular, Ref. 10 introduces broadband absorption asymmetry factor

$$\bar{J}_1 = (\sigma \, T_R^4)^{-1} \int_0^{\infty} J_1(\rho, m) \, E_\lambda(T_R) \, d\lambda, \qquad (7)$$

where T_R is the effective radiation temperature; $E_\lambda(T_R)$ is the Plank's function for absolutely black body; and $J_1(\rho, m)$ is the spectral asymmetry factor defined by equation (3).

Now we will consider gas kinetics aspects of aerosol evolution in the radiation field. In Ref. 11 it is shown that, in case of stationary droplet evaporation in gas-vapor mixture under the action of low-intensity field of directed radiation, the integrated evaporation rate can be represented as

$$\frac{dR_0}{dt} = -\frac{\rho_{1\infty}}{\rho_p} \left(\frac{2RT_\infty}{M_1}\right)^{1/2} \times$$

$$\times [(\beta - 1) \, G_\nu(\mathrm{Kn}) + G_\tau(\mathrm{Kn})] \, \langle T_s \rangle, \qquad (8)$$

where $\langle T_s \rangle$ is the mean droplet surface temperature given by

$$\langle T_s \rangle = T_\infty \left\{1 + \frac{1}{4} \, Q_{abs} \, I \Big/ \left[p_{1\infty} \, (2RT_\infty/M_1)^{1/2} \times \right.\right.$$

$$\left.\left. \times [(\beta - 1) \, (Q_\nu + \beta G_\nu) + Q_\tau + \beta G_\tau] + 4\varepsilon\sigma \, T_\infty^4 \right]\right\}, \qquad (9)$$

where T_∞ is the equilibrium temperature of gas mixture; $p_{1\infty}$ and $\rho_{1\infty}$ are pressure and density of vapor away from the particle; β is the latent heat of evaporation per molecule; the last term in the denominator accounts for radiative droplet cooling; G_ν, G_τ, Q_ν, and Q_τ are the kinetic coefficients that depend on Knudsen number. Thus, to calculate the absolute droplet evaporation rate in the radiation field, Q_{abs} must be known as a function of $m(\lambda)$ and ρ.

The nonuniformly heated particle in a rarefied gas is subject to photophoretic force of radiometric nature. In Ref. 8, the gas kinetics analysis is used to derive the formula for photophoretic force F_{ph}, valid in entire range of Knudsen numbers; it accounts for optical, thermophysical, and accommodation properties of aerosol particle and surrounding gas and has the form

$$F_{ph} = -\frac{2\pi}{3} \left(\frac{\pi M}{8RT_\infty}\right)^{1/2} \times$$

$$\times R_0^2 \, I J_1(\rho, m) \, F(\mathrm{Kn}, \Lambda, \alpha_E, \alpha_\tau, \alpha_n), \qquad (10)$$

where $F(\mathrm{Kn}, \Lambda, \alpha_E, \alpha_\tau, \alpha_n)$ is a complicated function of Knudsen number Kn, ratio Λ of particle and gas heat conductivities, and accommodation coefficients of momentum and energy of gas molecules on the particle

surface. Reference 8 presents a formula for velocity U_{ph} of photophoretic particle motion, which is proportional to J_1. The analysis of results shows that the direction of motion (sign of photophoresis) is entirely determined by the sign of J_1. The photophoresis sign cannot be changed by varying gas kinetics and accommodation parameters. Since the photophoresis strength and rate depend linearly on J_1, its numerical values also determine the absolute values of these characteristics. The photophoresis features of "volatile" particles also include, in addition to usual radiometric force, the jet force (caused by flow of evaporated matter from more heated fragments of the droplet surface), and thermocapillary force (arising due to temperature dependence of droplet surface tension coefficient). However, in this case the sign of J_1 determines the direction of particle motion.

Classification of atmospheric aerosols and particles' optical constants

The optical properties of atmospheric aerosol are determined primarily by its chemical composition and formation mechanism. Using the classification schemes of atmospheric aerosol (soil-erosion, marine, sulfate, and organic) as given in Refs. 12 and 13, as well as most reliable data on particle optical properties in a given wavelength range (such as provided by Ref. 14), it is possible to gain insight into what type of atmospheric aerosol particles and what aerosol optical properties are most suitable for initial analysis. These data were used here to calculate the studied microphysical optical characteristics.

Method of calculation of microphysical optical characteristics

The $B(\mathbf{r})$, Q_{abs}, J_1, and K_{rp} values were calculated from the Lorenz–Mie theory[5–7] as functions of refractive parameter for particles of different atmospheric aerosol types. Most reliable values of complex refractive index $m(\lambda)$ of particles were chosen for the wavelengths of solar spectrum. The internal field determines, through the Mie coefficients, the source function $B(\mathbf{r})$ as defined by Eq. (1) and factors Q_{abs} and J_1 as defined by Eqs. (2) and (3). We note that $B(\mathbf{r})$ is a strongly oscillating function of coordinates, especially for weakly absorbing particles; this degrades the accuracy of the two latter equations, and necessitates the use of direct numerical integration therein. For Q_{abs}, this problem is not new[5–7] and can be avoided by letting $Q_{abs} = Q_{ext} - Q_{sca}$, where Q_{ext} and Q_{sca} are dimensionless extinction and scattering cross sections, respectively.[7] Then Q_{abs} can be written as

$$Q_{abs} = 4J_0 = \frac{2}{\rho^2} \sum_{n=1}^{\infty} (2n+1) \times$$

$$\times [\mathrm{Re}\,(a_n + b_n) - (|a_n|^2 + |b_n|^2)], \qquad (11)$$

where a_n and b_n are the Mie coefficients.[7]

The expression for the asymmetry factor J_1, as in Ref. 10, after a little algebra was found to be

$$J_1 = -\frac{6nk}{|m|^2 \rho^3} \times$$

$$\times \mathrm{Im} \sum_{n=1}^{\infty} \left\{ \frac{n(n+2)}{m} (c_{n+1} c_n^* R_n + d_{n+1} d_n^* R_{n+1}) - \right.$$

$$\left. - \left[\frac{n(n+2)}{n+1} (c_{n+1} c_n^* + d_{n+1} d_n^*) + \frac{2n+1}{n(n+1)} d_n d_n^* \right] S_n \right\}, \qquad (12)$$

where the functions R_n and S_n are as they were defined in Ref. 10, and c_n and d_n are the Mie coefficients. The radiation pressure efficiency factor K_{rp} can be represented as

$$K_{rp} = Q_{abs} - \frac{4}{(kR_0)^2} \mathrm{Re} \sum_{n=1}^{\infty} \frac{n(n+1)}{2n+1} \times$$

$$\times \left[c_n b_n + \frac{n(n+2)^2}{2n+3} (c_n^* c_{n+1} + b_n^* b_{n+1}) \right]. \qquad (13)$$

The Mie coefficients were calculated using the well known Bohren and Huffman (BHMIE) scattering algorithm for a homogeneous sphere,[7] partially modified following recommendations of Ref. 6. In addition, we used the recommended algorithms of Barber and Hill ($S1$ and $S7$ codes[5]). The Mie coefficients, Q_{abs}, and K_{rp} computation error was controlled by comparison with data available in the literature.[6,15] The computations were made using mathematical software packages Mathematica 3.0 and Microsoft Fortran Power Station 4.0.

Discussion

The microphysical optical characteristics considered above were calculated for a wide class of particles of the main atmospheric aerosol types. As expected, two wide aerosol particle classes exist with distinct (i.e., weakly and strongly absorbing) properties. Water droplets (or water-bearing liquid-droplet aerosol particles) are most typical in the first class, and soot particles are most typical in the second one.

Water droplets. Figure 1*a* shows the source function $B(\mathbf{r})$ in the equatorial plane of the particle for a pure water droplet at $\rho = 12$ (calculations are made for $\lambda = 0.525$ μm, i.e., for spectral maximum of solar irradiance, and for $R_0 = 1$ μm). As seen, a spherical particle has the focusing effect, sometimes leading to more heating of the dark side, and to over 20 times higher intensity of the internal field than that of the incident radiation. The predominant heating of dark side at these wavelengths generally occurs for droplet radii from small-particle (Rayleigh) limit to geometric-optics region, though the small droplets have only slightly asymmetrical internal field (absorb fairly uniformly over their volume). As is well known,[4] all

characteristic features of absorption are manifested most clearly in the region of principal particle diameter. Such succinct description can be quite informative for a quantitative assessment of characteristics of local absorption.

Figure 1*b* shows the dependence of Q_{abs} on ρ; as seen, it has very jagged structure, generally called "ripples"[7] (to be distinguished from interference structure attributed to the focusing effect of the spherical particle). It is associated with the resonance electromagnetic modes of the spherical particles (Mie scattering resonances); typically, it becomes apparent for $\rho \geq 20$, where it has almost periodic structure. For larger droplets (tens of microns or larger), the use of Q_{abs} value calculated from Lorentz–Mie theory leads to a paradoxical result. Indeed, from equations (8) and (9), and from the characteristic Q_{abs} shape, it can be expected that the droplet evaporation rate in the field of directed radiation has a resonance dependence on droplet radius. However, no experimental support still exists for this speculation (see, e.g., Refs. 16 and 17). Rather, a resonance structure is revealed experimentally in the scattered light and is used to determine droplet size; at the same time, the evaporation rate is known to be a monotonic function. Most likely, this is due inertial character of thermal processes in the droplet interior and mass exchange on the droplet surface.

Possibly this is why the Q_{abs} estimates are frequently made using semiempirical relations, not immediately following from the strict Lorentz–Mie theory.[18] Among most successful approximations, widely used to estimate the absorbing properties of the water-bearing atmospheric aerosol, is the so-called Shifrin's formula[19]

$$Q_{abs}^{Sh} = \exp\{A\,[(n^2 + k^2)^{1/2} - 1]\}\,[1 - \exp(-4\rho k)], \quad (14)$$

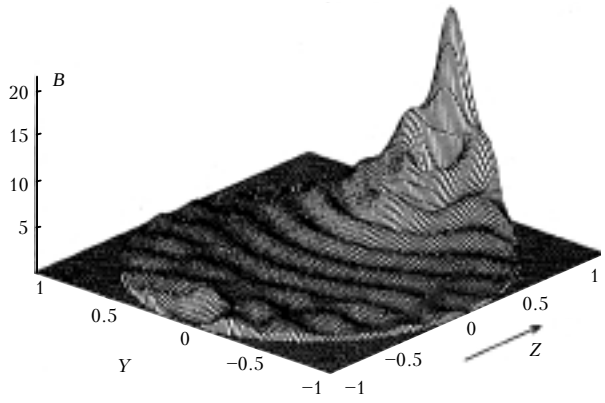

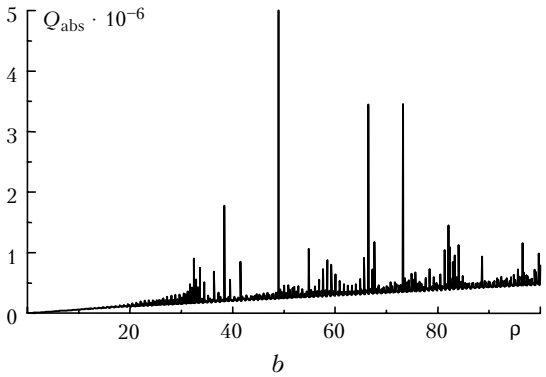

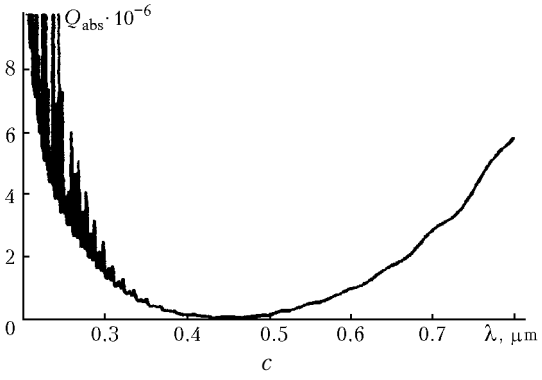

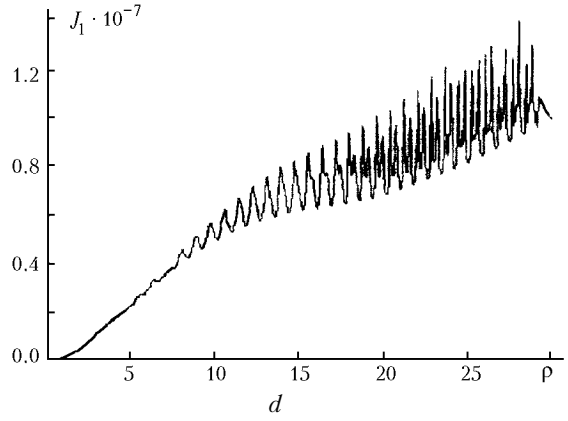

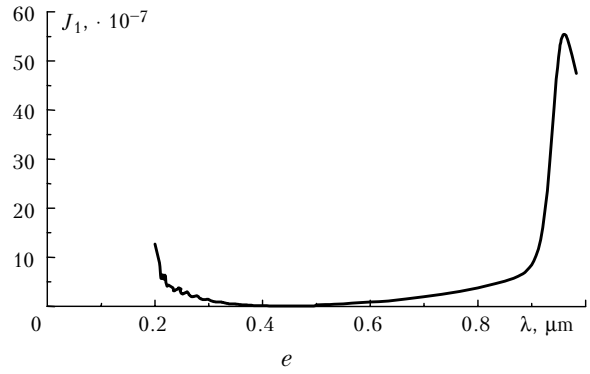

Fig. 1. Microphysical optical characteristics for pure water droplet at $\lambda = 0.525$ μm, $m = 1.334 + 1.32 \cdot 10^{-9}\,i$: source function $B(r, \theta, \phi = \pi/4)$ in particle equatorial plane for $\rho = 12$ ($R_0 = 1$ μm) (*a*); absorption efficiency factor Q_{abs} versus ρ (*b*); Q_{abs} versus λ for $R_0 = 1$ μm (*c*); absorption asymmetry factor J_1 versus refractive parameter ρ (*d*); and J_1 versus λ for $R_0 = 1$ μm (*e*).

where $A = -0.2$ as introduced originally by the author. We analyzed equation (14), and the analysis results were compared with the Lorentz–Mie computations; for $A = -0.2$, they were found to fit well the lower part of the envelope of Q_{abs} versus ρ curve calculated from the Lorentz–Mie theory. To account for the effect of Mie resonances on Q_{abs}, we also performed computations for $A = -0.444$. In this case, equation (14) approximates weighted mean Q_{abs} values with the account for resonances. Thus, Q_{abs}^{Sh} as defined by (14) can be interpreted as follows: it describes the effective absorption factor assumed to depend monotonically (without resonances) on the refractive parameter ρ.

As known,[7] the Mie scattering resonances have lower amplitude if nonmonochromatic radiation is incident on the spherical particle. These conditions are realized for water-bearing aerosol in the solar radiation field. For analysis of the non-chromaticity effect, we calculated Q_{abs} as a function of wavelength λ for fixed particle radii (curve in Fig. 1*c* is calculated for $R_0 = 1$ μm). The family of curves for different droplet radii has a few interesting features: (a) a rapid Q_{abs} increase for $\lambda \le 0.3$ μm (for $R_0 \ge 1$ μm, in this particle size range there are resonance peaks, disappearing for smaller particles); (b) a broad minimum in the wavelength region $\lambda \approx 0.3$–0.6 μm; and (c) the Q_{abs} increase for $\lambda > 0.7$–0.9 μm. We note that the minimum occurs at a wavelength corresponding to the spectral maximum of solar irradiance.

Figure 1*d* presents the dependence of asymmetry factor J_1 on the refractive parameter ρ. As seen, on the average, J_1 is an increasing function of ρ. Starting from $\rho \ge 5$, the resonance structure is clearly observed. It is less evident for non-monochromatic radiation, in which case J_1 is estimated, on the average, over a finite wavelength range [see equation (7)]. Obviously, for the asymmetry factor J_1, as for Q_{abs}, approximations of the type of Shifrin formula (14) would be very useful. Unfortunately, as far as we know, they are unavailable in the literature. For droplets of any size, J_1 is positive, though very small in absolute value ($\sim 10^{-7}$). According to equation (10), this means that water droplets can experience only negative photophoresis, i.e., they can move in the opposite direction to radiation propagation, at infinitesimal photophoretic speeds. This suggests that the photophoretic motion of water-bearing aerosol droplets can be neglected, for any particle size and any radiative intensity, not leading to the explosive droplet splitting.[1]

Quite different conclusion is drawn from analysis of absorption characteristics of oceanic water-bearing aerosol. As known, in the wavelength range of interest here the absorption coefficient of these aerosols may reach $k \approx 0.03$, well above that of pure water droplets. Correspondingly, Q_{abs} and J_1 have much higher absolute values for this aerosol. Figure 1*e* shows the J_1 versus λ plot for particle radius $R_0 = 1$ μm, which closely resembles the Q_{abs} versus λ plot for the same particle radius.

As numerical estimates showed, the radiation pressure force under conditions of low-intensity solar radiation cannot influence significantly the particle motion for any atmospheric aerosol type.

Soot particles. Soot particles are a subclass of strongly absorbing aerosols. The natural and anthropogenic soot is an important component of tropospheric and stratospheric aerosols, and it is present even at high arctic latitudes.[20] Assuming spherical symmetry (characteristic only of the initial soot particles formed by thermal destruction and combustion of carbon-bearing species), we calculated a series of aerosol characteristics mentioned above (Fig. 2). The soot particles exhibit strong absorption in the thin sunlit surface layer (Fig. 2*a*). Primarily, this is characteristic for quite large particles, whereas Rayleigh ones absorb uniformly over their volume, and may even have local peaks in the region of principal particle diameter for $\rho = 1$–3. Thus, the Lorentz–Mie calculations demonstrate only partial validity and applicability of the widespread thermodynamic model, assuming that an absolutely "black" particle absorbs all the incident radiation in the thin surface layer.[21]

Soot particles, compared with droplets, have completely different Q_{abs} versus ρ dependence (Fig. 2*b*). Specifically, the latter has no resonance structure and saturates to a constant level for large ρ. On the whole, Q_{abs} has very large absolute value. All attempts to approximate the Q_{abs} versus ρ dependence with a modified Shifrin formula had failed, and it is clearly why: by the principle of its construction, this formula is only applicable in the case of weakly absorbing water or water-bearing aerosols. The J_1 versus ρ dependence for soot also differs from that for droplets (Fig. 2*c*): again, it has no resonance structure, and saturates to the constant level $J_1 \approx -0.4$ toward large ρ values. For soot particles of any sizes, J_1 has negative sign, implying that only positive photophoresis (in direction of radiation propagation) can occur. For quite large soot particles, the absolute J_1 values are large, suggesting that strong photophoretic force can act on (and impart high speed) the particles.

Characteristic atmospheric aerosol types. Analogous calculations were also made for other atmospheric aerosol types. Analysis of calculation results shows that all main atmospheric aerosol types can be divided into two broad categories: the weakly and strongly absorbing particles. A criterion for inclusion in the first category is the smallness of the absorption coefficient k (quite roughly, it should be less than 0.03). Particles in this category have similar Q_{abs} versus ρ dependence to that of the pure water droplets (i.e., Q_{abs} increases with growing ρ, resonances are present for $\rho \ge 10$, and Q_{abs} have relatively small absolute values). This category includes

all oceanic and soil natural aerosol types. Also, the volcanic aerosol can be classified into this group. For these, a modified Shifrin formula can be used to approximate Q_{abs}. The J_1 versus ρ dependence for particles of this category is similar to that for pure water droplets (in that J_1 increases with growing ρ, resonances are present for $\rho \geq 5$, and absolute values are relatively small and positive).

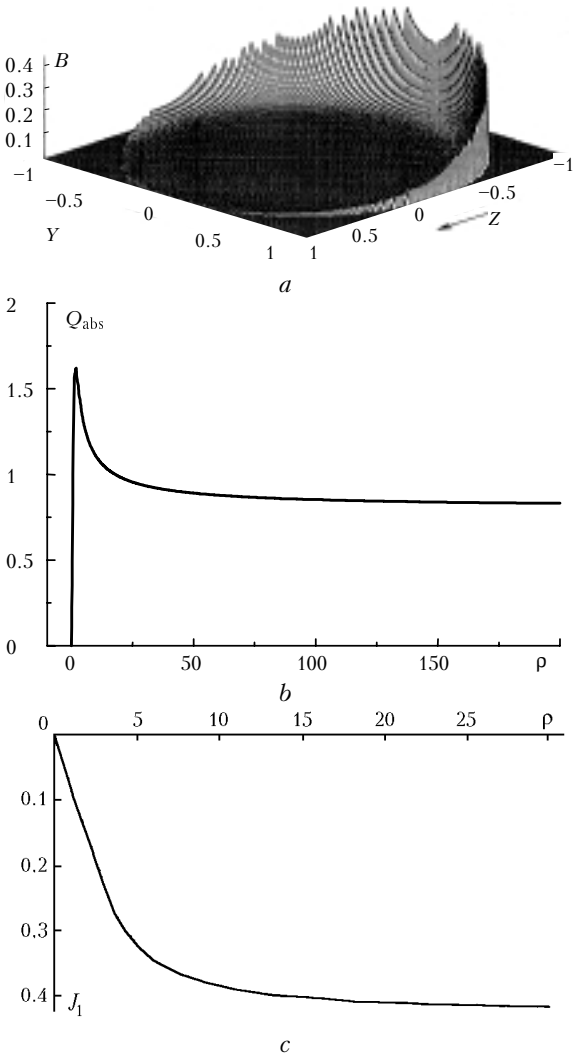

Fig. 2. Microphysical optical characteristics for soot particles at $\lambda = 0.500$ μm, $m = 1.82 + 0.7\,i$: source function $B(r, \theta, \phi = \pi/4)$ in equatorial particle plane for $\rho = 12$ ($R_0 \approx 1$ μm) (*a*); absorption efficiency factor Q_{abs} versus ρ (*b*); and absorption asymmetry factor J_1 versus refractive parameter ρ (*c*).

The category of strongly absorbing particles (behaving like soot particles) includes almost all aerosol classified into soil anthropogenic aerosol group (ash, industrial aerosol, etc.). Their characteristic feature is the rapid Q_{abs} increase, for $\rho \leq 2$, up to values frequently exceeding one, a subsequent smooth Q_{abs} decrease with growing ρ, the absence of resonances for large ρ, and large absolute Q_{abs} values. Generally, the modified Shifrin formula is inapplicable to this particle category. These particles typically have large negative J_1 values. A criterion for inclusion in this category is the large values of the refractive index n and absorption coefficient k (quite conventionally at $k \geq 0.3$). Lastly, moderately absorbing particles (i.e., those with quite large n and $0.03 \leq k \leq 0.3$) have asymmetry factor J_1 which: (*a*) in the presence of well-defined resonances, assumes quite large positive values until $\rho \approx 5$; (*b*) slowly decreases with sign reversal for $\rho \approx 10$–15; and (*c*) reaches large negative values with the further growth of ρ. Obviously, these particles will experience a photophoretic force reversal with a slow change of wavelength or, for a fixed wavelength, they will either move in the same or the opposite direction to radiation propagation, depending on the particle size. In particular, glycerin droplets (with $m = 1.57 + 0.03\,i$ at $\lambda = 10.63$ μm) possess these properties, and so they are widely used in the laboratory model studies.[22]

Conclusion

The paper presents preliminary results of theoretical analysis of absorbing properties of tropospheric and stratospheric aerosol. Main microphysical optical characteristics responsible for the dynamics of particles in the low-intensity radiation field are identified. Validity tests are made of the method for calculating these characteristics on the basis of Lorentz–Mie theory, that we plan to extend to analysis of other types of morphological types of single aerosol particles and particle ensembles. The obtained results will be used to construct stratospheric aerosol dynamics model with account of particle photophoresis, and to conduct and analyze the results of simulation of the processes of aerosol evolution in the radiation field by the methods of thermophysical model experiment[23] and electrodynamical microparticle suspension.[24]

Acknowledgments

The work is partially supported by the Russian Foundation for Basic Research (Grant No. 99–01–00143) and by the Department of Civil Engineering and Operations Research, USA (Grant No. 005).

References

1. V.E. Zuev, Yu.D. Kopytin, and A.V. Kuzikovskii, *Nonlinear Optical Effects in Aerosols* (Nauka, Novosibirsk, 1980), 184 pp.
2. O.A. Volkovitskii, Yu.S. Sedunov, and L.P. Semenov, *Propagation of High-Intensity Laser Radiation in Clouds* (Gidrometeoizdat, Leningrad, 1982), 312 pp.
3. V.I. Bukaty, I.A. Sutorikhin, V.N. Krasnopevtsev, et al., *Influence of Laser Radiation on Solid Aerosol* (Publishing House of Altai State University, Barnaul, 1994), 196 pp.
4. A.P. Prishivalko, *Optical and Thermal Fields Light inside Scattering Particles* (Nauka i Tekhnika, Minsk, 1983), 190 pp.

5. P.W. Barber and S.C. Hill, *Light Scattering by Particles: Computational Methods* (World Scientific Publ., Singapore, 1990), 261 pp.
6. G.M. Aivazyan, *Propagation of Millimeter and Submillimeter Waves in Clouds. Handbook* (Gidrometeoizdat, Leningrad, 1991), 480 pp.
7. K. Bohren and D. Huffman, *Light Absorption and Scattering by Small Particles* (Mir, Moscow, 1986), 664 pp.
8. S. Beresnev, V. Chernyak, and G. Fomyagin, Phys. Fluids **A5**, No. 8, 2043–2052 (1993).
9. E. Lloyd, U. Lederman, and Yu.N. Tyurin, eds., *Handbook of Applied Statistics* (Finansy i Statistika, Moscow, 1989), Vol. 1, 510 pp.
10. D.W. Mackowski, Int. J. Heat Mass Transfer **32**, No. 5, 843–854 (1989).
11. V.G. Chernyak, Izv. Akad. Nauk SSSR, Ser. Fiz. Atmos. Okeana **31**, No. 6, 800–808 (1995).
12. K.Ya. Kondrat'ev, N.I. Moskalenko, and D.V. Pozdnyakov, *Atmospheric Aerosol* (Gidrometeoizdat, Leningrad, 1983), 224 pp.
13. L.S. Ivlev and S.D. Andreev, *Optical Properties of Atmospheric Aerosols* (Publishing House of Leningrad State University, 1986), 360 pp.
14. V.M. Zolotarev, V.N. Morozov, and E.V. Smirnova, *Optical Constants of Natural and Technical Media. Handbook* (Khimiya, Leningrad, 1984), 216 pp.
15. I.L. Zel'manovich and K.S. Shifrin, *Tables on Light Scattering*. Vol. 3. *Extinction, Scattering, and Radiation Pressure Coefficients* (Gidrometeoizdat, Leningrad, 1968), 432 pp.
16. E.J. Davis, P. Ravindran, and A.K. Ray, Chem. Eng. Commun. **5**, 251–268 (1980).
17. G. Sageev, R.C. Flagan, J.H. Seinfeld, and S. Arnold, J. Colloid Interface Sci. **113**, No. 2, 412–429 (1986).
18. A.A. Kokhanovsky and E.P. Zege, J. Aerosol Sci. **28**, No. 1, 1–21 (1997).
19. K.S. Shifrin, Trudy Gl. Geofiz. Obs., No. 109, 179–190 (1961).
20. V.P. Shevchenko, A.P. Lisitsyn, A.A. Vinogradova, et al., Atmos. Oceanic Opt. **13**, Nos. 6–7, 510–533 (2000).
21. L.D. Reed, J. Aerosol Sci. **8**, No. 2, 123–131 (1977).
22. S. Arnold and M. Lewittes, J. Appl. Phys. **53**, No. 7, 5314–5319 (1982).
23. A.I. Bogolepov, P.E. Suetin, S.A. Beresnev, Teplofizika Vysokikh Temperatur **34**, No. 5, 751–756 (1996).
24. V.A. Runkov, P.E. Suetin, and S.A. Beresnev, "Electromagnetic Suspension with Circular Electrodes for Aerosol Study," VINITI, No. 239–B00, February 3, 2000, Moscow, (2000), 15 pp.